High Ethylene Production through ODHE Membrane Reactors based on Fast Oxygen-Ion Conductors

Dr. M. Pilar Lobera, Sonia Escolástico, Dr. José M. Serra*

Instituto de Tecnología Química (UPV-CSIC). Universidad Politécnica de Valencia. Consejo Superior de Investigaciones Científicas. Avenida de los Naranjos s/n.46022 Valencia, Spain

ChemCatChem 3 (2011) 1053-1058

(doi: 10.1002/cctc.201100055)

Abstract

High ethylene productivity through the oxidative dehydrogenation of ethane has been achieved in a catalytic membrane reactor based on a highly solid-state oxygen permeable material ($Ba_{0.5}Sr_{0.5}Co_{0.8}Fe_{0.2}O_{3-\delta}$). Ethylene is selectively produced by avoiding the direct contact of molecular oxygen and hydrocarbons and therefore minimizing the oxygen concentration in the reaction side. Another key aspect in the process is the dilution of the ethane in the feed to achieve high ethylene yields. There exists a specific combination of the ethane concentration and feed flow, which maximizes ethylene productivity, while the diluting gas nature has a direct impact on the formation of higher olefins and coking issues. Indeed, the use of methane as almost-inert dilutant allows reducing oligomerization and aromatization of the formed ethylene and therefore improving the reactor stability even at operating temperatures from 800-900 ºC. This behavior is attributed to the competitive adsorption of methane and ethane/ethylene, the modification of the radical-driven homogeneous reaction and the change of partially-reducible membrane surface. The achieved productivity values at 850ºC were 383 mL min^{-1} cm^{-2} (Ar) and 353 mL min^{-1} cm^{-2} (CH_4), with a selectivity of 80 % (Ar) and 90 % (CH_4), respectively.

Keywords: Ethylene; membrane reactor; BSCF; MIEC membrane; perovskite; ODHE

*corresponding author: Dr. J.M. Serra, e-mail: jmserra@itq.upv.es, Fax: +34963877809

1. Introduction

Ethylene is a key intermediate product in industrial chemistry. The principal current method for its production is steam cracking of ethane, naphtha or heavier feedstocks (usually carried out at T > 800 ºC), which is energy intensive. Moreover, it involves side reactions as coke formation, thus discontinuous operation is necessary for reactor clean-up. A potential alternative to steam cracking is the oxidative dehydrogenation of ethane (ODHE). This process is exothermic, while dehydrogenation and cracking are endothermic, so energy efficiency is improved and the presence of oxygen prevents coke formation. However, the use of pure oxygen or enriched air contributes to increase process cost and the coexistence of ethane and gaseous O_2 leads to undesired combustion reactions [1-5]. In the last years, several catalysts and reactors systems have been tested [2-4] in ODHE reaction, although for an industrial implementation an ethylene productivity greater than 1 $g_{C_2H_4}\ g_{cat}^{-1}\ h^{-1}$ should be required [6]. However, the membrane reactor technology allows overcome the ODHE drawbacks.

Dense mixed ionic-electronic conductors (MIEC) membranes show good oxygen permeability at elevated temperatures without the need of external electrical currents with a theoretical separation selectivity of 100%. The highest oxygen flux is generally observed for dense ionic membranes having a cubic perovskite structure, typically at high temperature above 800 ºC [7, 8]. Bulk oxygen species diffuse via oxygen vacancies in the crystal lattice from oxygen rich side to reaction side. Surface oxygen species are formed on the reaction side, which would react with the ethane. Thus, the use of dense MIEC membranes allows preventing the direct contact between the ethane and molecular oxygen, which allows (1) preventing the use of explosive gas mixtures; and (2) minimizing the formation of carbon oxides due to direct reaction between hydrocarbons and oxygen, thus higher selectivities of ethylene can be expected.

In this context, dense MIEC membrane reactors are highly attractive solutions for ODHE process intensification, since both, separation (oxygen-ion diffusion through the perovskite lattice) and reaction are integrated in the same unit [5, 9-11]. Mirodatos and co-workers [5] reported an ethylene yield of 76 % at 777 ºC, with a reactor using as membrane a dense MIEC ($Ba_{0.5}Sr_{0.5}Co_{0.8}Fe_{0.2}O_{3-\delta}$) with Pd cluster deposited. Akin and Lin [9] reported an ethylene yield of 56 % (per pass) with a dense tubular ceramic membrane reactor made of $Bi_{1.5}Y_{0.3}SmO_3$ at 875 ºC. Yang et al.[10] reported an ethylene selectivity of 80 % at 84 % ethane conversion by using a dense MIEC ($Ba_{0.5}Sr_{0.5}Co_{0.8}Fe_{0.2}O_{3-\delta}$) as membrane in a co-feed reactor. Caro et al.[11] investigated the ODHE using a dense perovskite hollow fiber membrane compared with the performance of a disk-shaped membrane and the best results were obtained with the last one (~ 67 % ethylene yield).

Ethane is typically produced by separation of natural gas (on average 4-5 % of *wet gas* on the mass basis). This is a type of natural gas, which contains more ethane, propane and heavier gases that dry gas, which is nearly pure methane, and by recovery from refinery gases. In consequence, for a potential industrial application of ODHE process might be interesting to consider the use of methane as a dilutant, thus avoiding additional steps as separation process.

The present work aims to study systematically the influence of the operating conditions on the ODHE reaction performed on a catalytic membrane reactor based on a solid-state oxygen permeable material ($Ba_{0.5}Sr_{0.5}Co_{0.8}Fe_{0.2}O_{3-\delta}$). Special attention will be paid to the use of very high specific gas flow rates in the reaction chamber in order to achieve high ethylene productivity. The variables under study included the feed concentration of ethane (reaction chamber), the specific feed flow rate in reaction chamber and operating temperature. Finally, it is investigated the influence of the kind of gas used for ethane dilution in the feed stream. Specifically, it is studied the effect of diluting with argon and methane.

2. Experimental

2.1 Membrane preparation and characterization

Preparation of membranes samples was performed using $Ba_{0.5}Sr_{0.5}Co_{0.8}Fe_{0.2}O_{3-\delta}$ (BSCF) powder provided by IKTS Fraunhofer (Germany). The powder was ball-milled in acetone suspension in order to decrease the grain size obtained prior pelletizing. Then, the membrane was prepared by uniaxial pressing at 150 kN. The densification of the disk was achieved by sintering in air for 5 h at 1100 ºC (2 ºC min^{-1} ramp).

XRD was carried out on a Philips X'Pert Pro equipped with an X'celerator detector using monochromatic Cu Kα radiation. XRD patterns were recorded in the 2θ range from 20 to 90 ºC and analysed using X'Pert Highscore Plus software (PANalytical).

2.2 Membrane reactor set-up and ODHE experiments

Oxygen permeation studies and catalytic test were carried out in the same reactor set-up. The quartz reactor was inside an electrical furnace. The temperature was measured by a thermocouple close to the surface membrane (reaction side). A PID controller maintained temperature variations within 2 ºC of the set point.

The measurements were performed on 15 mm diameter disks. The sample consisted of a gastight ~ 0.8 mm thick BSCF disk sintered. Sealing was done using gold gaskets. Oxygen was separated from a mixture of synthetic Air-N_2. The reaction side was fed either by argon or diluted methane as sweep gas (in the oxygen permeation test) or a

mixture of ethane and the corresponding sweep gas (in the ODHE experiments). Permeate was analyzed by on-line gas chromatography using micro-GC Varian CP-4900 equipped with Molsieve5A, Pora-Plot-Q glass capillary, and CP-Sil modules. All feed streams were individually mass flow controlled. Membrane gas leak free conditions were ensured by monitoring nitrogen concentration on the products gas stream. Data reported are achieved at steady state after one hour on reaction stream and each test has been repeated three times to minimize analysis error, obtained an experimental analytical error below 0.5 %.

3. Results and discussion

3.1 Oxygen permeation

Oxygen permeation flux through the MIEC membrane is a key aspect in ODHE reaction, determining the performance of the catalytic membrane reactor. From the oxygen content measured in sweep side of the permeation assemble, the argon flow rate and the area of the membrane surface exposed to the flowing gas, the total oxygen permeation rate, $J(O_2)$ (mL min^{-1} cm^{-2}), was calculated. Figure 1 shows the temperature dependence of oxygen permeation flux through the BSCF membrane. It could reach 2.0 mL min^{-1} cm^{-2} at 1273 K with a pO_2=0.21 atm in the oxygen-rich chamber. This value is higher than the oxygen permeation flux (1.0 mL min^{-1} cm^{-2}) for the practical applications specified by Bouwmeester[7]. Oxygen permeation flux is 2.5-fold increased when diluted methane (15% in Ar) is used as sweep gas. This aspect was expected due to the increase in the separation driving force, i.e., log pO_2 (air)/pO_2 (sweep) from 0.88 to 3.85[I] when diluted methane is used as sweep gas. A significant flux increase is also expected when the inlet gas flow rare is increased due to the overcome of concentration polarization limitations [12].

From a mechanistic point of view, oxygen transport through a dense MIEC material involves the surface-exchange reaction on the membrane surface and bulk-diffusion of charged species and electron/electron holes in the bulk phase. Generally, each of these steps could be the rate limiting, according to the reactor design, mode of operation, and properties of the membrane material. The slowest step is expected to limit the overall oxygen permeation rate. The BSCF membranes may present a change in the limiting step as a function of the temperature range and the membrane thickness [5, 8]. In both oxygen permeation tests performed with different sweep gas, there was a change of slope with an increasing temperature. The apparent activation energies (E_a) were

[I] Here, it is considered the ideal case in which it is assumed that the permeate pO_2 corresponds to the sweep gas (diluted methane). For the Wagner equation integration, it is also assumed that ionic conductivity does not depends significantly on pO_2 and this is negligible with respect to the electronic conductivity.

calculated by Arrhenius equation. At higher temperatures –zone ①–, the process is controlled by bulk-diffusion and the apparent activation energy is the same in both cases (~ 35 kJ mol^{-1}). But when the process is controlled by surface exchange reactions (at lower temperatures –zone ②–), the apparent activation energy change from 65 kJ mol^{-1} (argon as sweep gas) to 80 kJ mol^{-1} (diluted methane as sweep gas). The fact that the E_a is constant at high temperature regardless of the applied driving force confirms that the oxygen permeation is limited by the bulk transport and the mechanism is not changed although the oxygen vacancy concentration does. On the other hand, the change of the activation energy ascribed to the surface oxygen exchange suggests that the active sites for oxygen adsorption, reduction and dissociation have been altered by the strong pO_2 variation. Indeed, the use of diluted methane as sweep gas induces (a) a severe change in the surface vacancy concentration and (b) the reduction of redox species, i.e. Fe and Co cations, involved in the oxygen activation.

3.2 ODHE performances

Figure 2 shows the ethylene productivity and ethylene yield as a function of the flow rate in the reaction chamber (Q_{Feed}). A larger residence time in the reaction side (lower flow rates) often means a higher probability of oxidation of the valuable intermediate produced and this leads to a decrease of ethylene selectivity and an increase of ethane conversion. Thus, the ethylene yield slightly changed and passed through a maximum at a Q_{Feed} of 400 mL min^{-1}. The maximum is due to the opposite evolution of selectivity and yield with increasing residence time. The high C_2H_4 yield may be related to the fact that the O_2/C_2H_6 ratio was close to the stoichiometric value. It is worth mentioning that a high C_2H_4 yield value is obtained even for a very high flow rate (500 mL min^{-1}). Moreover, the ethylene productivity increased monotonically with the Q_{Feed} in the range of operating condition studied, i.e., with an increase in the amount of ethane fed in the reactor.

In order to analyze the influence of the ethane concentration in the reaction feed stream, diverse tests were carried out keeping constant the residence time and varying the ethane concentration in the reaction mixture for three different operating temperatures (800, 825 and 850 ºC). In this experiment (Figure 3 and 4), a very high feed flow rate (Q_{Feed} = 550 mL min^{-1}) was used. In all cases, ethane conversion decreases with the ethane concentration in the feed mixture while the ethylene selectivity hardly changes (Figure 3). On the other hand, for a given feed composition, the ethane conversion increases with the reaction temperature, while the selectivity slightly declined and remained always at high values (~ 80-90%). This small selectivity decrease is principally ascribed to radical-driven oligomerization reactions and in a lesser extent to deep hydrocarbon oxidation and aromatization (See Table 1). This change in the selectivity is in agreement with previous reports using similar membrane reactors [5, 11]. Figure 4 shows the corresponding ethylene productivity as a function of ethane concentration in the reaction mixture for three different temperatures. It is also

plotted the ethylene productivity for an ideal yield value of 100%. These results demonstrate the potential of high temperature catalytic membrane reactors since extremely high ethylene productivity values can be achieved. Specifically, the ethylene productivity increased when the ethane concentration in the reaction mixture was raised; and a maximum value of ethylene productivity was reached when ~ 80 % C_2H_6 was fed at 850 °C (383 mL_{C2H4} min^{-1} cm^{-2}; with an ethylene selectivity of 80.1 %). The minimization of secondary reactions, i.e. oligomerization and aromatization, at high temperatures and very high ethylene concentrations has been probably achieved by the use of very high flow rates (lower residence times). Consequently, the appropriate fluid dynamics regime in the reactor [13] allowed the rapid extraction (quenching) of the produced ethylene from the hot membrane surface and the reaction chamber while the high temperature allowed the high oxygen permeability and a high catalytic activity.

When the operation temperature is increased, the ODHE reaction goes from a just catalytic process to a gas-phase reaction through a stage in which the two processes get involved in a hetero-homogeneous regime. Several studies suggest that the thermal gas-phase ethane dehydrogenation is likely to be operative at higher temperatures [14-18]. However, in the MIEC membrane reactors, the chemistry of membrane surface reactions would play an important role and it is not clear whether ODHE reaction occurs in the gas-phase or in the catalytic regime at these temperatures. Different works indicate that catalytic processes take place in the ethylene formation, such as ethyl radical formation due to the existence of superficial oxygen species. Moreover, the *in situ* detection of ethyl radicals in the gas-phase imply that once formed, these radicals are partially delivered into the gas-phase [18]. The formation of the radical is the rate determining step and the further faster radical decomposition to form ethylene could take place either on the catalyst surface or in the gas phase. The oxygen permeation process enables (1) the formation of the radical through the reaction of ethane with lattice oxygen to form an oxygen vacancy and (2) the radical decomposition to form water instead of molecular hydrogen.

To evaluate the contribution of gas-phase reaction and catalytic processes in a MIEC reactor, different experiments have been performed using the same experimental set-up. Two different membrane reactors were tested in the same operating conditions; i.e. an inert membrane of Al_2O_3 disc and a BSCF membrane. Figure 5 shows the ethylene yield as a function of the ethane concentration in the reaction mixture, for the different membrane reactors studied. In the case of the inert membrane, only the gas-phase reaction take places and it is observed that increasing the amount of oxygen co-fed in the reaction chamber, the ethylene yield decreases due to the formation of CO_x. The use of O_2-free feed led to the rapid formation of carbon deposits in the membrane reactor set-up. Moreover the ethylene yield obtained with the MIEC membrane reactor is higher than that achieved when only the gas-phase reaction occurs. These results suggest that at

high temperature, the ODHE reaction goes through gas-phase reactions but in a MIEC membrane reactor an important catalytic contribution takes place. The ODHE reaction would proceed via ethyl radical formation on the surface of the MIEC membrane, released as ethylene into the gas phase, due to the existence of active oxygen species on the MIEC membrane surface. Additionally, the MIEC membrane reactor allows minimizing the formation of coke.

As mentioned before, it might be interesting to consider the use of methane as a dilutant for a potential industrial application of ODHE process. In order to study the effect of the dilutant used in the reaction mixture, some tests were performed using methane or argon as diluting agent while maintaining constant the rest of operating conditions (Table 2). Although the presence of methane has a negative effect on ethane conversion, it was possible to achieve higher ethylene selectivity values than those achieved by using argon as dilutant. Specifically, a significant decrease of C_4^+ formed during the ODHE reaction was observed (Table 1 and S2).

Regarding the ethylene productivity, when methane was used as diluted instead of argon, a maximum ethylene productivity (see Figure 6a) of 356 mL min^{-1} cm^{-2} was achieved with an ethylene selectivity of 90.6 %, when ~ 80 % C_2H_6 was fed (Q_{Feed} = 550 mL min^{-1}) at 850 °C. Since the oligomerization and aromatization reactions were reduced, the subsequent ethylene separation steps might be easier (Figure 6a-b). A similar effect of methane dilution has been reported by Machocki et al., [19] for simultaneous reaction of OCM and ODHE in a co-feed fixed-bed reactor. This behaviour is attributed to competitive adsorption on the membrane surface between methane and ethane /ethylene, the reduction of the gas-phase ethyl radical lifetime, and the modification of the membrane surface that is partially reduced.

The catalytic membrane reactor stability was assessed for several days although it is well-know that BSCF is prone to carbonate in the presence of CO_2 at temperatures below 850 ºC. Post-mortem SEM analysis of the membrane surface (reaction side) indicates the formation of secondary phases, i.e., Ba-Sr carbonates, on the grain boundary (See Figures S2 – S4). For the short operation time, the oxygen permeation was not influenced by the formation of these first carbonate domains. For a durable and robust operation, a membrane material or composite arrangements with higher stability against carbonation and phase transition should be used. Possible candidates are doped $SrFeO_3$, La_2NiO_4 and CeO_2 based membranes or multilayer composite membranes [20-23].

4. Conclusion and outlook

Oxidative dehydrogenation of ethane has been studied on a catalytic membrane reactor based on a dense oxygen-ion conducting membranes made of BSCF. The membrane arrangement allows avoiding the direct contact of molecular oxygen and hydrocarbons[II] and consequently high ethylene selectivity is achieved. Moreover, the use of the membrane reactor allowed attaining very high ethylene productivities (383 mL min^{-1} cm^{-2} when using argon as ethane dilutants) due to combination of (1) adequate fluid dynamics which enables the proper feed contact with the membrane and the rapid quenching of the formed ethylene; and (2) the high activity due to the high temperature and the active oxygen species diffusing through the membrane. Furthermore, the ethane dilution with methane instead of argon allows: (1) reducing the extent of ethylene oligomerization, aromatization and coking reactions, (2) maximizing the productivity at a certain ethane feed concentration (~ 80%), and (3) improving substantially the membrane reactor stability even at operating temperatures from 800-900 ºC.

In conclusion, the use of the MIEC membranes provides a promising alternative to conventional ethylene production. The synergy between oxygen permeation, catalytic oxidation and fluid dynamics at the membrane surface and reactor chamber is supposed to be responsible for the obtained exceptional results. The use of catalytic coatings in the MIEC membranes may allow improving the present results, e.g. decreasing the operating temperature, increasing the C_2H_4 yield, etc. Moreover, the deposition of a ceria-based thin protective layers on perovskite membranes may increase the long-term stability of the membrane under realistic operating conditions[24]. This concept may open new perspectives in advanced catalysis for several reactions of selective oxidation, and yet represents another challenge. This membrane reactor system can be applied for other oxidative dehydrogenation reactions such as propane or butane dehydrogenation, although the catalyst and reaction conditions should be carefully adjusted due to the higher reactivity of these alkanes and the produced olefins/polyolefins in order to prevent oligomerization and coking issues.

Acknowledgements

Financial support by the Spanish Ministry for Science and Innovation (Project ENE2008-06302 and FPI Grant JAE-Pre 08-0058), EU through FP7 NASA-OTM Project (NMP3-SL-2009-228701), and the Helmholtz Association of German Research Centres through the Helmholtz Alliance MEM-BRAIN (Initiative and Networking Fund) is kindly acknowledged.

[II] The oxygen concentration in the reaction products stream is always significantly below 100 ppm. See Table 1 in Supporting Material.

References

[1] M. M. Bhasin *Topics in Catalysis*. **2003**, 23, 145-149.
[2] T. Blasco, J. M. L. Nieto *Applied Catalysis A:General*. **1997**, 157, 117-142.
[3] F. Cavani, N. Ballarini, A. Cericola *Catalysis Today*. **2007**, 127, 113-131.
[4] R. K. Grasselli *Catalysis Today*. **1999**, 49, 141-153.
[5] M. Rebeilleau-Dassonneville, S. Rosini, A. C. van Veen, D. Farrusseng, C. Mirodatos *Catalysis Today*. **2005**, 104, 131-137.
[6] X. F. Lin, C. A. Hoel, W. M. H. Sachtler, K. R. Poeppelmeier, E. Weitz *Journal of Catalysis*. **2009**, 265, 54-62.
[7] H. J. M. Bouwmeester *Catalysis Today*. **2003**, 82, 141-150.
[8] J. Sunarso, S. Baumann, J. M. Serra, W. A. Meulenberg, S. Liu, Y. S. Lin, J. C. D. da Costa *Journal of Membrane Science*. **2008**, 320, 13-41.
[9] F. T. Akin, Y. S. Lin *Journal of Membrane Science*. **2002**, 209, 457-467.
[10] H. H. Wang, Y. Cong, W. S. Yang *Catalysis Letters*. **2002**, 84, 101-106.
[11] H. H. Wang, C. Tablet, T. Schiestel, J. Caro *Catalysis Today*. **2006**, 118, 98-103.
[12] S. Baumann, J. M. Serra, M. P. Lobera, S. Escolástico, F. Schulze-Küppers, W. A. Meulenberg *Journal of Membrane Science.* **2011 (Accepted Manuscript)** doi: 10.1016/j.memsci.2011.04.050
[13] J. M. Gozálvez-Zafrilla, A. Santafé-Morós, S. Escolásico, J. M. Serra *Journal of Membrane Science*. **2011 (Accepted Manuscript)**, doi: 10.1016/j.memsci.2011.05.016.
[14] P. J. Gellings, H. J. M. Bouwmeester *Catalysis Today*. **2000**, 58, 1-53.
[15] A. Julbe, D. Farrusseng, C. Guizard *Catalysis Today*. **2005**, 104, 102-113.
[16] F. Klose, M. Joshi, C. Hamel, A. Seidel-Morgenstern *Applied Catalysis A:General*. **2004**, 260, 101-110.
[17] G. A. Martin, C. Mirodatos *Fuel Processing Technology*. **1995**, 42, 179-215.
[18] E. Morales, J. H. Lunsford *Journal of Catalysis*. **1989**, 118, 255-265.
[19] A. Machocki, A. Denis *Chemical Engineering Journal*. **2002**, 90, 165-172.
[20] D. F. C. Mirodatos, A.C. van Veen, M. Rebilleau-Dassonneville, A. Abrutis, A., Teiserskis in Method for preparing supported electron and ionic oxygen conducting ultra thin dense membranes, Vol. WO2006024785 (A1) (Ed.^Eds.: Editor), City, **2006**.
[21] C. M. Chen, D. L. Bennett, M. F. Carolan, E. P. Foster, W. L. Schinski, D. M. Taylor in *ITM Syngas ceramic membrane technology for synthesis gas production, Vol. Volume 147* (Eds.: B. Xinhe, X. Yide), Elsevier, **2004**, pp.55-60.
[22] C. Delbos, G. Lebain, N. Richet, C. Bertail *Catalysis Today*. **2010**, 156, 146-152.
[23] J. M. Serra, V. B. Vert, O. Buchler, W. A. Meulenberg, H. P. Buchkremer *Chemistry of Materials*. **2008**, 20, 3867-3875.
[24] I. García-Torregrosa, M. P. Lobera, C. Solís, P. Atienzar, J. M. Serra *Advanced Energy Materials*. **2011 (Accepted Manuscript)**, doi: 10.1002/aenm.201100169.

TABLES

Table 1. Catalytic performance of BSCF-based membrane for the ODHE reaction. Methane-free basis.

					CH_4 as sweep gas				Ar as sweep gas			
T (ºC)	Q_{Feed} (mL(STP) min^{-1})	Q_{Air} (mL(STP /min^{-1})	O_2 (% v/v)	C_2H_6 (% v/v)	X_{C2H6} (%)	S_{C2H4} (%)	S_{C3+} (%)	S_{C4+} (%)	X_{C2H6} (%)	S_{C2H4} (%)	S_{C3+} (%)	S_{C4+} (%)
850	414	210	4.0	1.0	46.7	72.48	0.42	0	93.8	74.17	0	3.14
850	414	210	4.0	2.3	43.3	82.48	0.34	0.83	92.2	83.82	0.46	8.22
850	414	210	4.0	3.5	42.6	88.11	0.45	1.51	90.8	84.67	0.32	10.91
850	414	210	4.0	4.3	42.4	89.93	0.46	2.02	90.0	84.71	0.38	11.59
850	414	210	4.0	5.4	41.9	90.90	0.49	2.88	89.3	84.91	0.27	12.15
850	414	210	4.0	7.5	40.0	92.48	0.50	3.90	87.6	84.81	0.42	13.00
800	550	200	5.0	70	42.3	93.56	0.55	5.83	46.9	91.77	0.62	6.88
800	550	200	5.0	80	39.9	93.71	0.47	5.74	45.3	90.85	1.07	7.54
800	550	200	5.0	85	36.5	93.64	0.40	5.83	43.3	90.72	1.00	7.51
850	550	200	5.0	70	69.1	91.16	0.51	8.11	82.0	84.72	1.46	13.25
850	550	200	5.0	80	70.3	91.50	0.45	7.74	83.2	84.81	1.54	13.35
850	550	200	5.0	85	67.7	89.57	0.45	9.59	82.5	83.90	1.60	14.08

FIGURE CAPTIONS

Figure 1. Oxygen permeation flux through BSCF membrane measured as a function of temperature (Arrhenius plot). Synthetic air (21 % v/v O_2); different sweep gases.

Figure 2. Ethylene productivity as a function of feed flow rate in the reaction side. T = 850 ºC, 5.4 % C_2H_6 in Ar, 4.0 % O_2, Q_{Air} = 210 mL(STP) min^{-1}.

Figure 3. Ethane conversion and ethylene selectivity obtained as a function of the ethane concentration in the reaction side. Q_{Feed} = 550 mL(STP) min^{-1}, 5.0 % O_2, ethane diluted with argon. Q_{Air} = 200 mL(STP) min^{-1}.

Figure 4. Ethylene productivity reached as a function of the percentage of ethane in the reaction side. Q_{Feed} = 550 mL(STP) min^{-1}, 5.0 % O_2.

Figure 5. Ethylene yield obtained in inert membrane reactor and BSCF membrane reactor. T = 850 ºC, Q_{Feed} = 400 mL(STP) min^{-1}, ethane diluted with argon.

Figure 6. Ethylene productivity reached as a function of the percentage of ethane in the reaction side. (a) High ethane feed concentration level while ethane was diluted with methane or argon and Q_{Air} = 200 mL(STP) min^{-1}, 5.0 % O_2, Q_{Feed}= 550 mL(STP) min^{-1}; and (b) low ethane feed concentration level while ethane was diluted with methane or argon and Q_{Air} = 210 mL(STP) min^{-1}, 4.0 % O_2, Q_{Feed}= 400 mL(STP) min^{-1}.

Figure 1

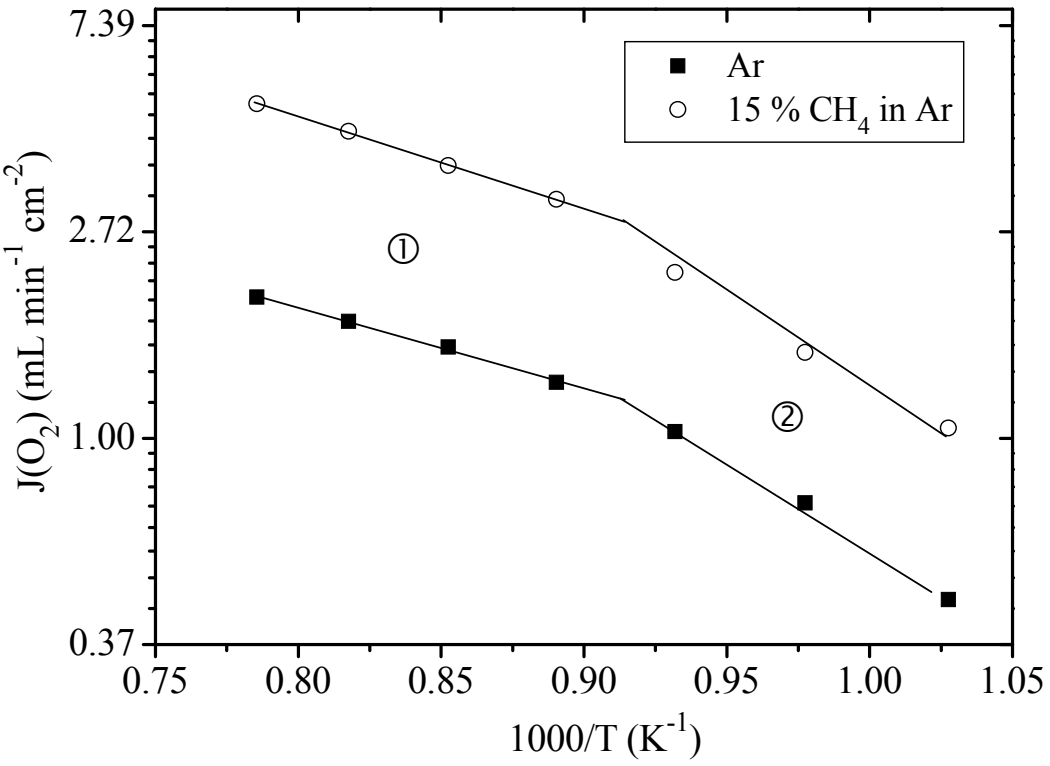
7.39
2.72
1.00
0.37
0.75
0.80
0.85
0.90
0.95
1.00
1.05
J(O2) (mL min-1 cm-2)
1000/T (K-1)
Ar
15 % CH4 in Ar
①
②

Figure 2

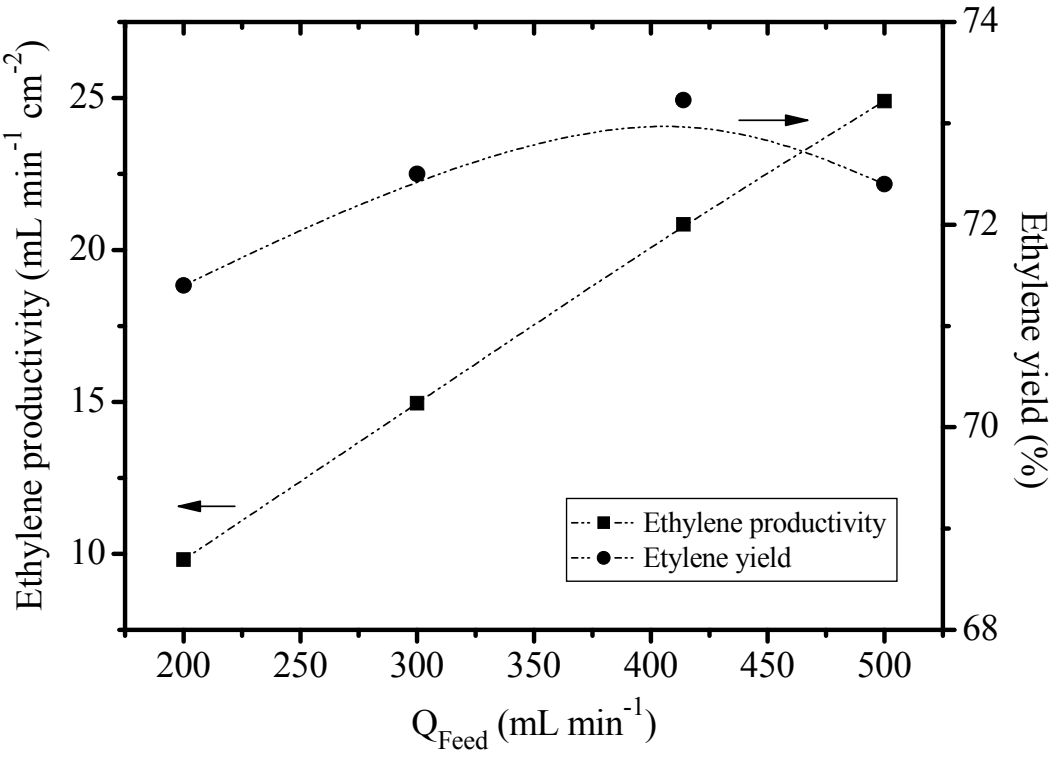
Ethylene productivity (mL min-1 cm-2)
Ethylene yield (%)
QFeed (mL min-1)
Ethylene productivity
Etylene yield
10
15
20
25
68
70
72
74
200
250
300
350
400
450
500

Figure 3

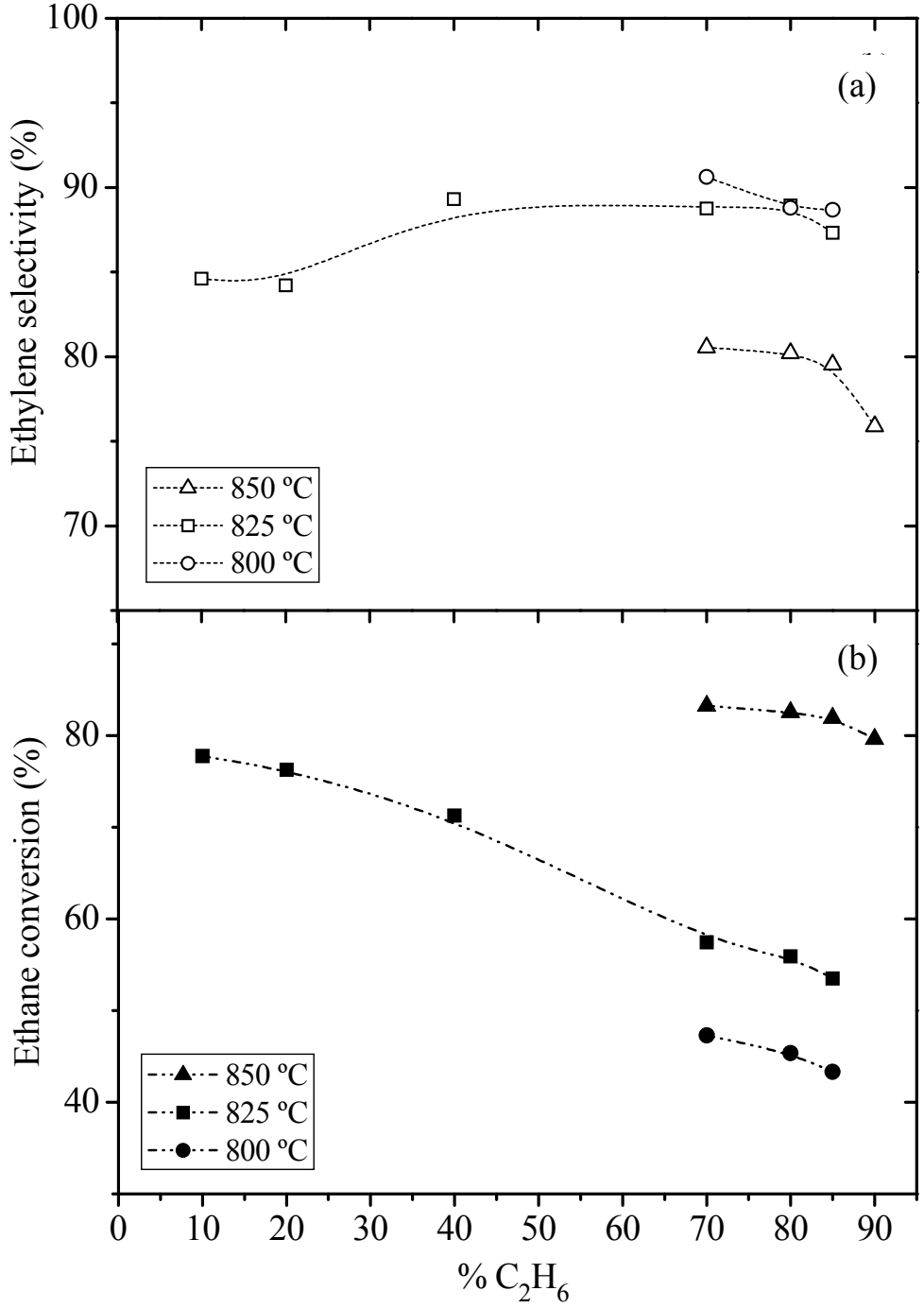
(a)
Ethylene selectivity (%)
100
90
80
70
850 ºC
825 ºC
800 ºC
(b)
Ethane conversion (%)
80
60
40
850 ºC
825 ºC
800 ºC
0
10
20
30
40
50
60
70
80
90
% C_2H_6

Figure 4

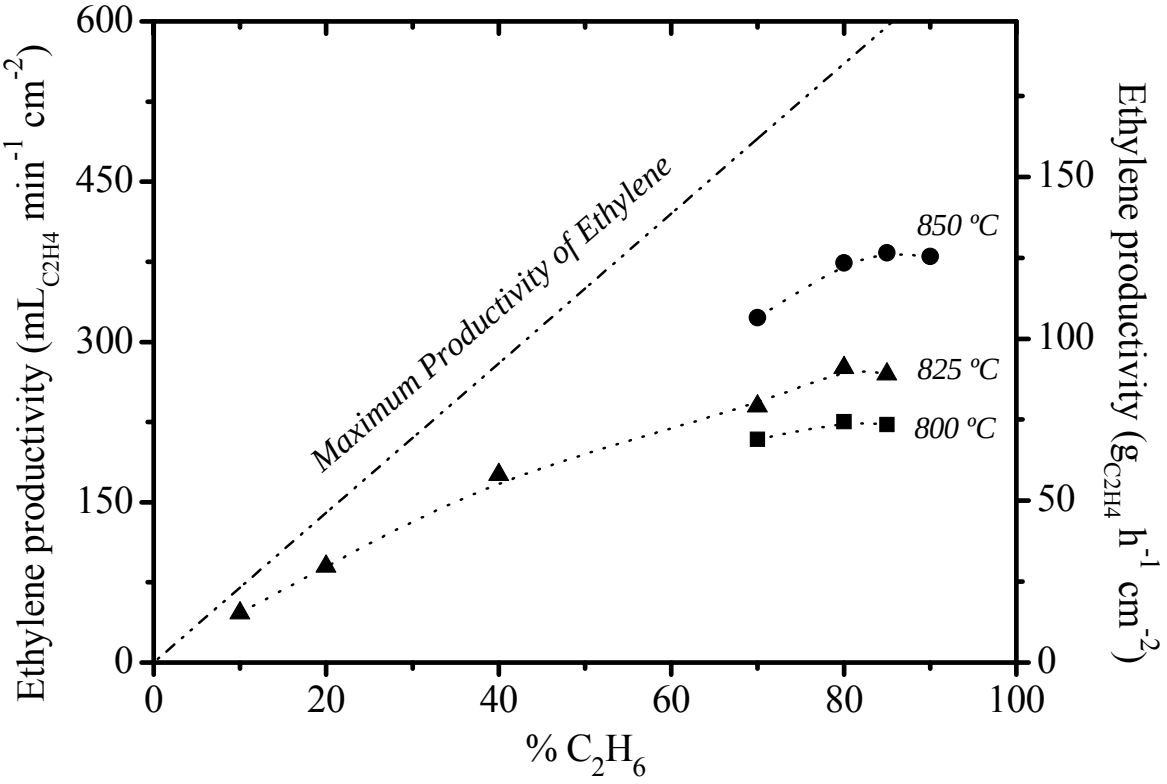
Ethylene productivity (mL_{C2H4} min^{-1} cm^{-2})
Ethylene productivity (g_{C2H4} h^{-1} cm^{-2})
% C_2H_6
Maximum Productivity of Ethylene
850 ºC
825 ºC
800 ºC
0
150
300
450
600
0
50
100
150
0
20
40
60
80
100

Figure 5

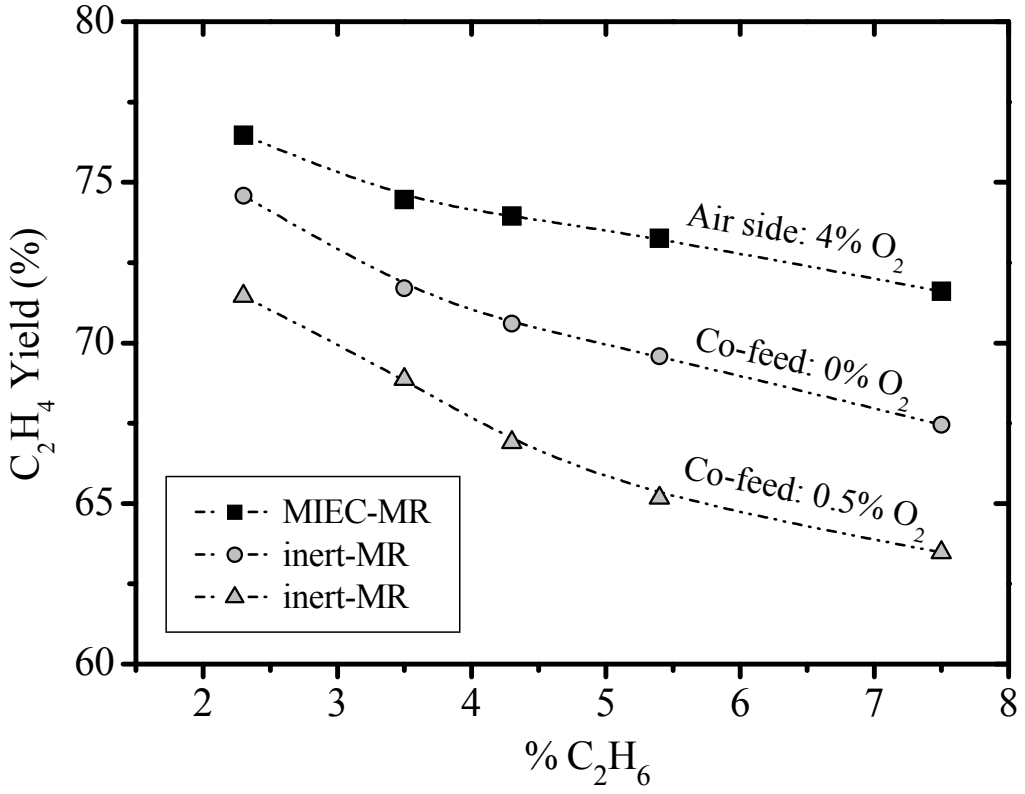
80
75
70
65
60
2
3
4
5
6
7
8
C_2H_4 Yield (%)
% C_2H_6
Air side: 4% O_2
Co-feed: 0% O_2
Co-feed: 0.5% O_2
MIEC-MR
inert-MR
inert-MR

Figure 6

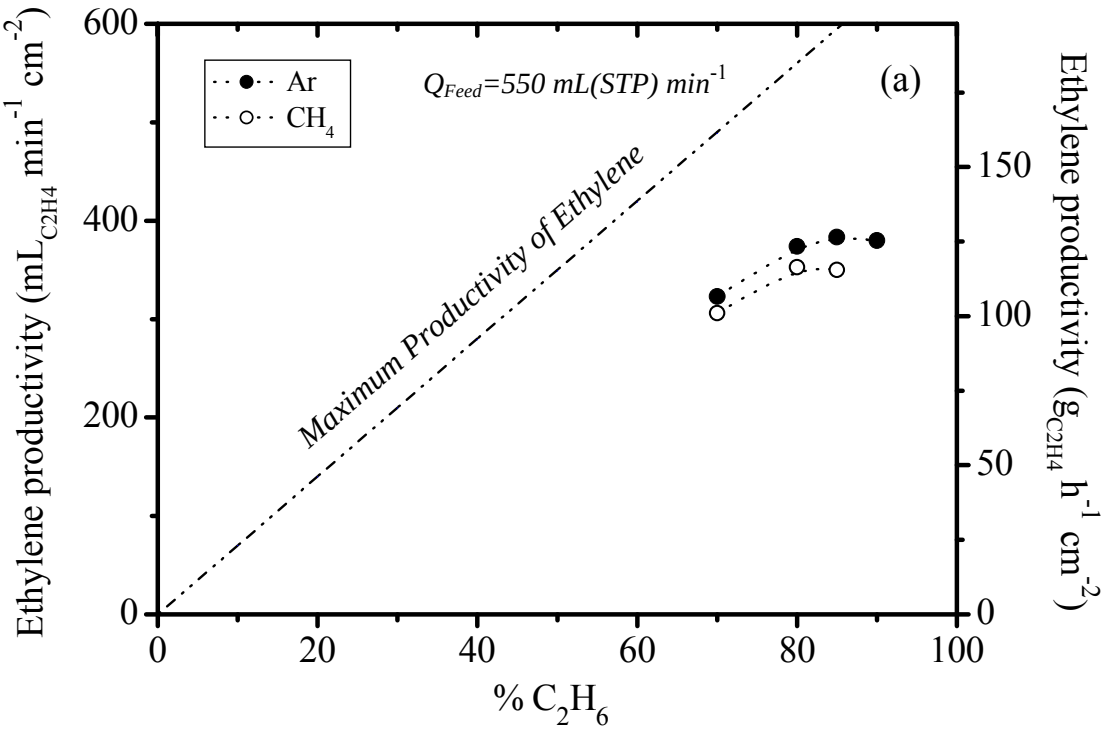
Ethylene productivity (mL_{C2H4} min^{-1} cm^{-2})
Ethylene productivity (g_{C2H4} h^{-1} cm^{-2})
% C_2H_6
Ar
CH_4
Q_{Feed}=550 mL(STP) min^{-1}
(a)
Maximum Productivity of Ethylene
0
200
400
600
0
50
100
150
0
20
40
60
80
100

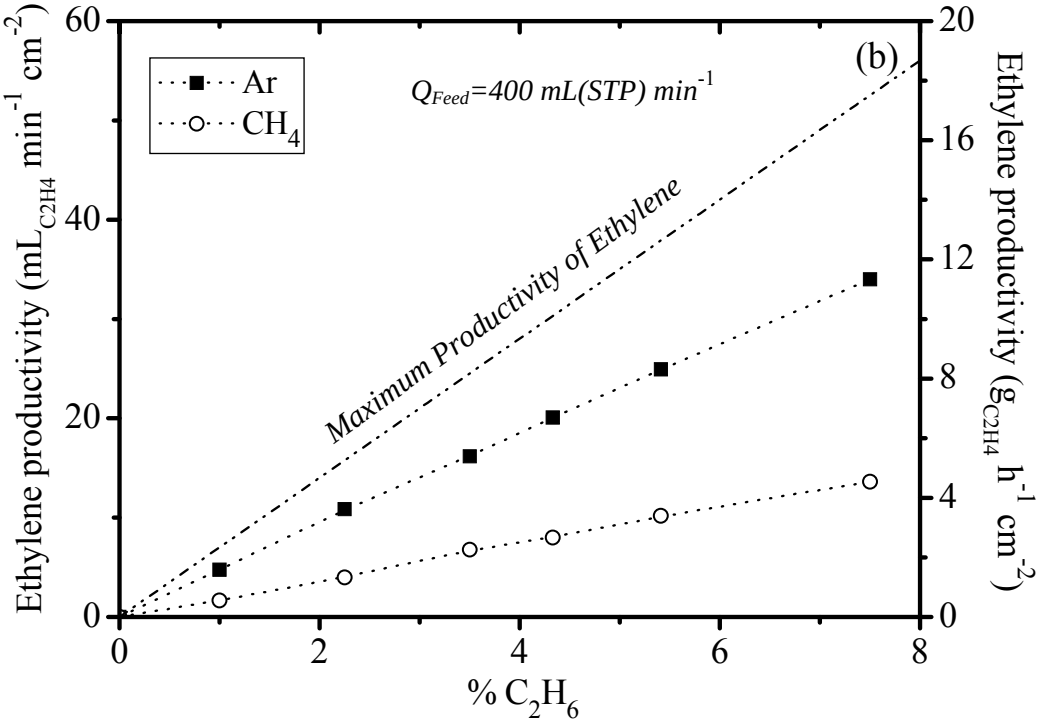
Ethylene productivity (mL_{C2H4} min^{-1} cm^{-2})
Ethylene productivity (g_{C2H4} h^{-1} cm^{-2})
% C_2H_6
Ar
CH_4
Q_{Feed}=400 mL(STP) min^{-1}
(b)
Maximum Productivity of Ethylene
0
20
40
60
0
4
8
12
16
20
0
2
4
6
8

Supporting Information

from “High Ethylene Production through ODHE Membrane Reactors based on Fast Oxygen-Ion Conductors” by M. Pilar Lobera, Sonia Escolástico, José M. Serra*

doi: 10.1002/cctc.201100055

Figure S1

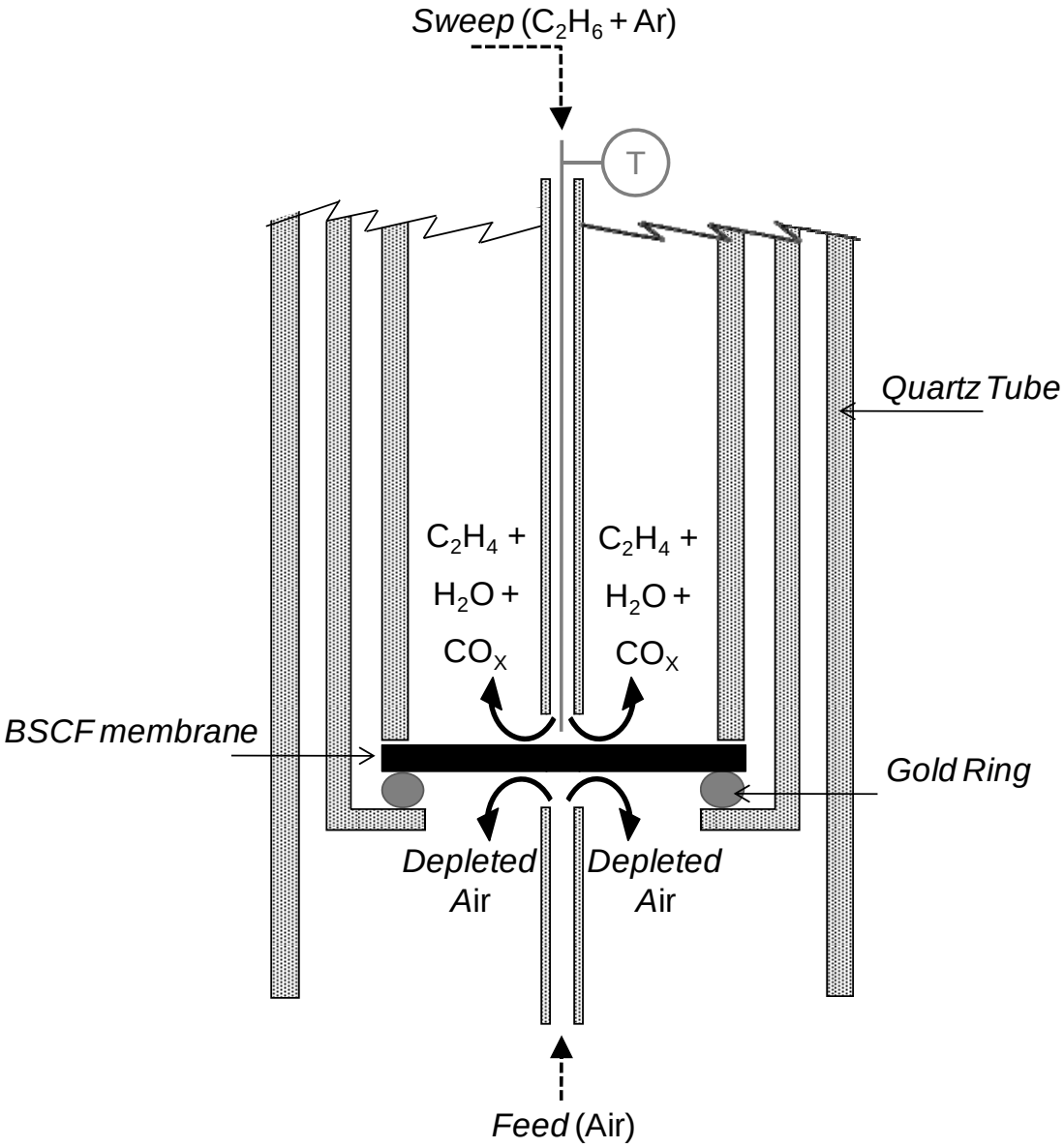

-.Schematic of the quartz membrane reactor design.-

Figure S2

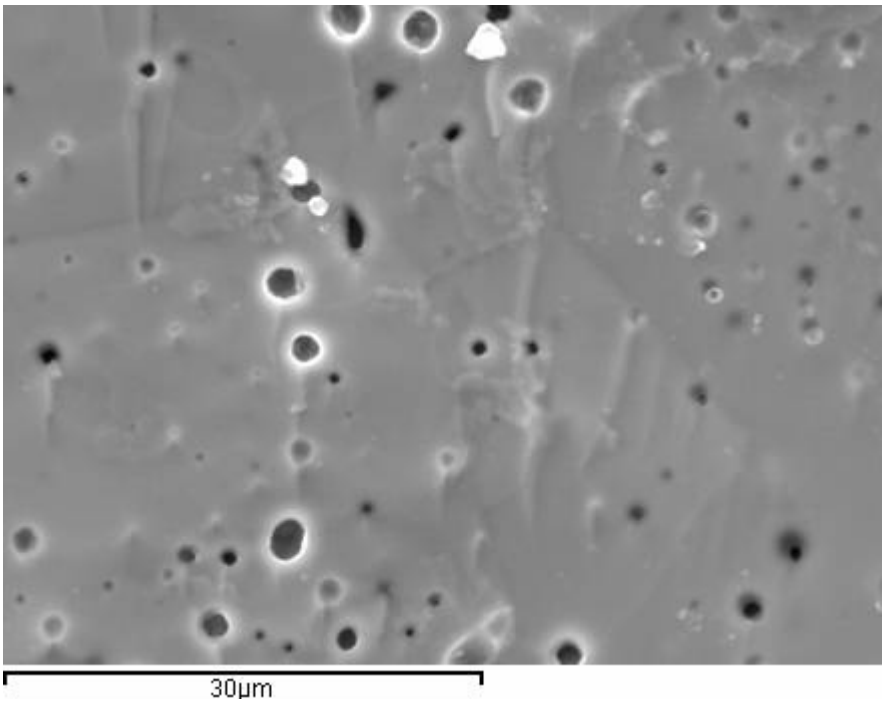

-.SEM picture of the fracture cross-section of $Ba_{0.5}Sr_{0.5}Co_{0.8}Fe_{0.2}O_{3-\delta}$ *(BSCF) membrane before catalytic tests.-*

Figure S3

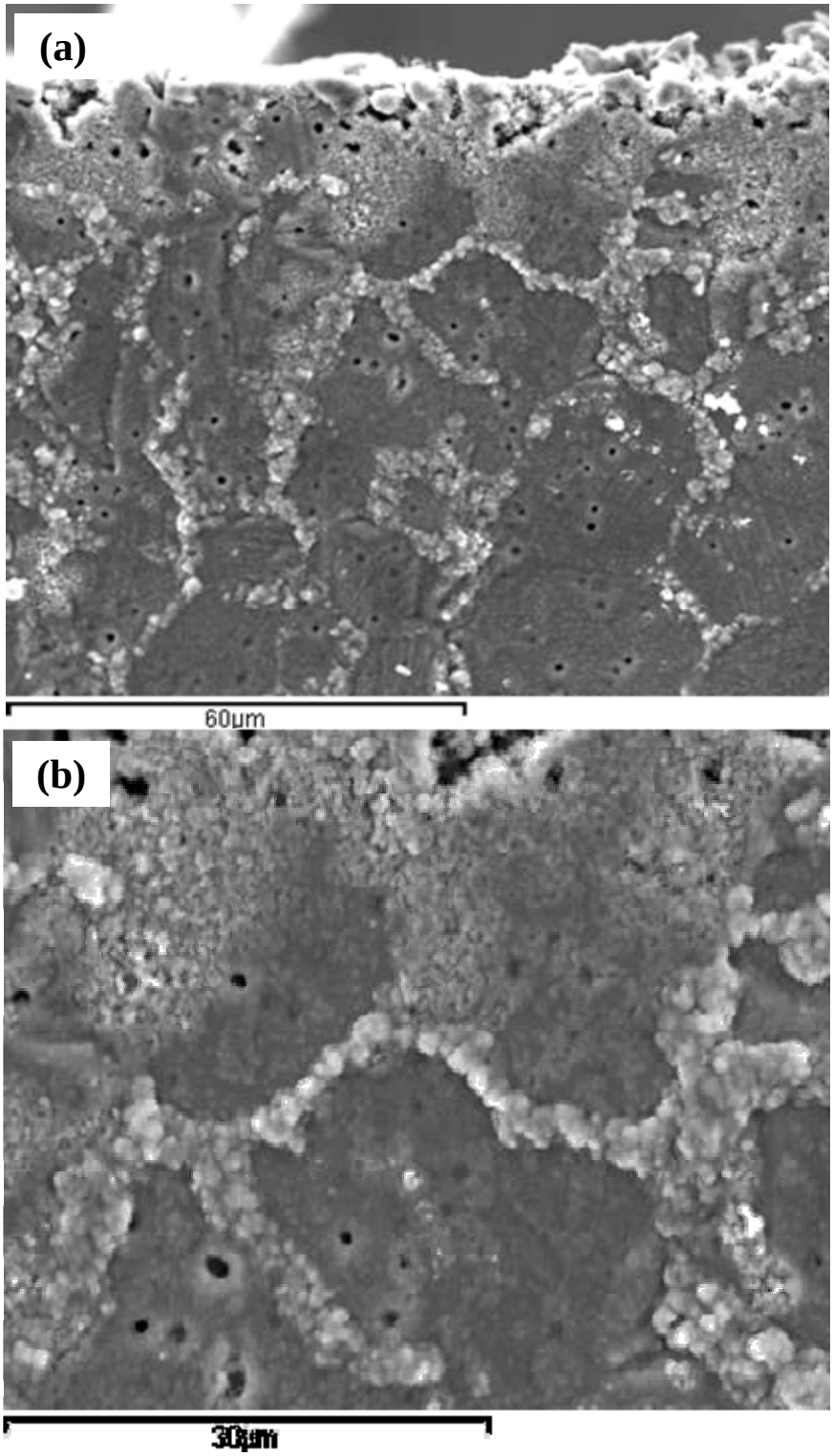

-.SEM pictures of the fracture cross-section of $Ba_{0.5}Sr_{0.5}Co_{0.8}Fe_{0.2}O_{3-\delta}$ (BSCF) membrane after catalytic tests. (a) Membrane surface on the reaction side. (b) The analyzed area corresponds to the closest to the reaction side surface.-

Figure S4

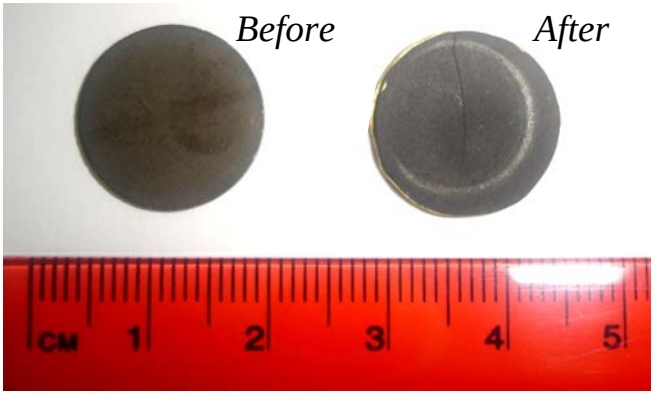

-Picture of the $Ba_{0.5}Sr_{0.5}Co_{0.8}Fe_{0.2}O_{3-\delta}$ (BSCF) membrane before and after catalytic tests.-

Figure S4

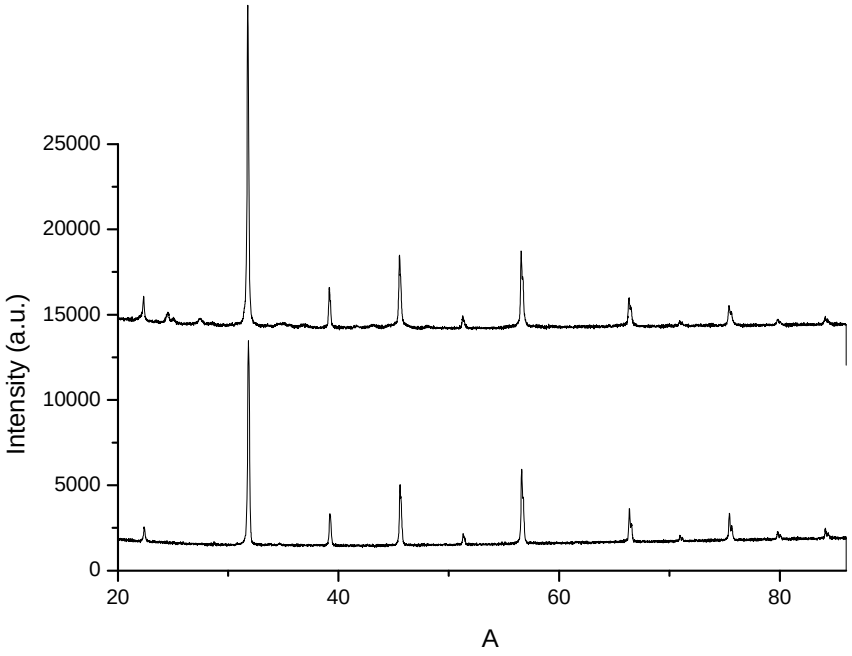

-. *XRD patterns of the membrane* $Ba_{0.5}Sr_{0.5}Co_{0.8}Fe_{0.2}O_{3-\delta}$ *(BSCF) after (top) and before (bottom) the catalytic tests. The XRD analysis was carried out on the membrane surface corresponding to the reaction chamber.*

Table S1. O_2 concentration (ppm) in the permeate. Q_{Feed} = 550 mL min^{-1}, Q_{air}=200 mL min^{-1}.

	[O_2] in ppm		
% C_2H_6	800 ºC	825 ºC	850 ºC
70	33	34	47
80	34	40	49
85	36	39	53
90			55

Table S2. Catalytic performance of BSCF-based membrane for the ODHE. Methane-free basis.

					CH_4 as sweep gas							***Ar as sweep gas***						
T *[ºC]*	***Q_{Feed}*** *[mL min^{-1}]*	***Q_{Air}*** *[mL min^{-1}]*	***O_2*** *[% v/v]*	***C_2H_6*** *[% v/v]*	***X_{C2H6}*** *(%)*	***S_{C2H4}*** *(%)*	***S_{C3+}*** *(%)*	***S_{C4+}*** *(%)*	***[a]C_6H_6***	***% H_2***	***% CO***	***X_{C2H6}*** *(%)*	***S_{C2H4}*** *(%)*	***S_{C3+}*** *(%)*	***S_{C4+}*** *(%)*	***[a]C_6H_6***	***% H_2***	***% CO***
850	414	210	4.0	1.0	46.7	69.0	0.4	0.0	nd	2.5	0.17	93.8	72.0	0.0	3.0	nd	1.7	0.23
850	414	210	4.0	2.3	43.3	77.8	0.5	0.7	nd	2.9	0.20	92.2	81.3	0.4	8.0	538	3.9	0.18
850	414	210	4.0	3.5	42.6	84.4	0.6	1.5	nd	4.1	0.24	90.8	82.0	0.4	10.6	849	6.1	0.14
850	414	210	4.0	4.3	42.4	82.8	0.6	1.8	nd	4.9	0.21	90.0	82.0	0.4	11.3	1226	7.1	0.13
850	414	210	4.0	5.4	41.9	85.6	0.6	2.7	nd	6.7	0.21	89.3	82.1	0.5	11.7	1792	8.9	0.13
850	414	210	4.0	7.5	40.0	86.5	0.6	3.7	556	9.8	0.16	87.6	81.8	0.5	12.5	2452	11.8	0.11
800	550	200	5.0	70	42.3	91.9	0.5	5.7	4432	23.5	0.02	46.9	90.6	0.6	6.9	5510	19.6	0.17
800	550	200	5.0	80	39.9	92.8	0.5	5.6	4715	24.2	0.03	45.3	88.8	1.1	7.2	5706	21.6	0.17
800	550	200	5.0	85	36.5	93.3	0.4	5.8	5187	24.8	0.02	43.3	88.6	1.1	7.3	5988	22.4	0.20
850	550	200	5.0	70	69.1	90.3	0.5	8.0	14146	30.5	0.02	82.0	80.5	1.4	12.6	22633	29.4	0.21
850	550	200	5.0	80	70.3	90.6	0.4	7.8	15088	32.6	0.03	83.2	80.1	1.5	12.7	26207	32.7	0.19
850	550	200	5.0	85	67.7	89.1	0.5	9.5	16503	36.1	0.18	82.5	82.5	1.5	12.8	35365	35.1	0.21

[a] ppm